

Angular dependence of ferromagnetic resonance linewidth in thin films

J. Dubowik, K. Załęski, and H. Głowiński

Institute of Molecular Physics, Polish Academy of Sciences, PL-60-179 Poznań, Poland

I. Gościańska

Department of Physics, A. Mickiewicz University, Umultowska 85, PL-61-614 Poznań, Poland

(Received 29 December 2010; revised manuscript received 14 November 2011; published 29 November 2011)

We comment on a frequently applied analysis of an out-of-plane angular dependence of the ferromagnetic resonance linewidth ΔH in thin films. Using an expanded Suhl's formula for the field-swept linewidth, we show that the angular dependence of ΔH in a number of thin magnetic films is well described as a sum of two terms only: an intrinsic contribution and an extrinsic one due to Gilbert damping and two-magnon scattering, respectively. For some special cases (e.g., films with perpendicular anisotropy), an additional term of inhomogeneous broadening due to local variations in the out-of-plane anisotropy may be required.

DOI: [10.1103/PhysRevB.84.184438](https://doi.org/10.1103/PhysRevB.84.184438)

PACS number(s): 76.50.+g, 75.40.Gb, 75.70.-i

I. INTRODUCTION

The out-of-plane angular dependence of the ferromagnetic resonance linewidth ΔH in field-swept (with the microwave frequency ω kept constant and a varied applied field H) ferromagnetic resonance (FMR) experiments has often been analyzed in order to obtain some additional information on the intrinsic contribution to the linewidth ΔH^{Gilb} due to the Gilbert damping and on the extrinsic contributions resulting from structural inhomogeneity and defects present in thin magnetic films.¹ The analysis requires, however, an exact transformation from the frequency-swept linewidth $\Delta(\omega/\gamma)$ to the field-swept ΔH one. For an infinite isotropic ferromagnet, such a transformation is straightforward,²

$$\Delta\left(\frac{\omega}{\gamma}\right) = \Delta H = 2\alpha\left(\frac{\omega}{\gamma}\right), \quad (1)$$

where the frequency-swept linewidth $\Delta(\omega/\gamma)$ is expressed in the units of the field and γ is the gyromagnetic ratio. However, in thin films, the magnetization M and the field H are not collinear in a broad range of the field angle Θ_H and hence³

$$\Delta\left(\frac{\omega}{\gamma}\right) = \frac{d(\omega/\gamma)}{dH} \Delta H(\Theta_H). \quad (2)$$

The term $\Delta(\omega/\gamma)$ expresses the full linewidth at half maximum (FWHM) characteristic of FMR absorption. Equation (2) leads to Suhl's formula⁴ for the peak-to-peak linewidth,

$$\Delta H_{\text{pp}}(\Theta_H) = \frac{\alpha}{\sqrt{3}} \frac{P(\Theta_H) + Q(\Theta_H)}{\frac{d(\omega/\gamma)}{dH}}, \quad (3)$$

where $P(\Theta_H) = \frac{1}{M \sin^2(\Theta)} E_{\Phi\Phi}$ and $Q(\Theta_H) = \frac{1}{M} E_{\Theta\Theta}$ are the second partial derivatives of the anisotropic part of the magnetic free-energy density E with respect to the spherical coordinates Φ and Θ of the magnetization M in the Smit-Beljers⁵ relation, which have to be determined numerically together with the equilibrium condition for magnetization M .⁶ Since Eq. (3) expresses the peak-to-peak linewidth from absorption derivative, $\sqrt{3}$ is included.

The derivative in the denominator of Eq. (3) has been more⁶⁻¹² or less^{3,13-16} properly treated in a number of papers.

Additionally, calculations of the full derivative are cumbersome in the case of additional anisotropic parts of the magnetic free-energy density, which may lead to artificially increase^{17,18} some contributions to the linewidth in a frequently applied approach^{14-16,18} referred to as a local resonance model.^{19,20} In this model, applied for the first time by Chappert *et al.*²¹ for the films with perpendicular anisotropy, it is assumed that the field-swept linewidth is usually described by a series of contributions $\Delta H = \Delta H^{\text{Gilb}} + (\partial H/\partial \Theta_H) \Delta \Theta_H + (\partial H/\partial H_i) \Delta H_i$, where $\Delta \Theta_H$ and ΔH_i represent variations of Θ_H and H_i due to orientation distribution of independent grains (mosaicity) and internal field, respectively. While this approach may be applicable for the films with a strong perpendicular anisotropy,²¹⁻²⁴ in thin films with a high magnetization and small inhomogeneities, it has no physical basis since inhomogeneities are effectively smoothed by dipolar and exchange interactions.¹⁹ In this case, the two-magnon model²⁰ is more pertinent than the local resonance model and the frequency-swept linewidth is a sum of the intrinsic (Gilbert) $\Delta(\omega/\gamma)^{\text{Gilb}}$ and extrinsic (two-magnon) $\Delta(\omega/\gamma)^{2\text{mag}}$ contributions,

$$\Delta\left(\frac{\omega}{\gamma}\right) = \Delta\left(\frac{\omega}{\gamma}\right)^{\text{Gilb}} + \Delta\left(\frac{\omega}{\gamma}\right)^{2\text{mag}}. \quad (4)$$

Our comment is concerned with such a transformation—a procedure of separation of these contributions to $\Delta H(\Theta_H)$ as well as of proper transformations $\Delta H^{\text{Gilb}}(\Theta_H) \rightarrow \Delta(\omega/\gamma)^{\text{Gilb}}$ and $\Delta H^{2\text{mag}}(\Theta_H) \rightarrow \Delta(\omega/\gamma)^{2\text{mag}}$ for the case of ultrathin magnetic films with a negligible exchange-conductivity damping, which is independent of Θ_H .¹

II. FMR LINEWIDTH IN THIN FILMS

Equations (2) and (3) may be solved with full derivatives, but it is more convenient to express $\Delta(\omega/\gamma)$ as

$$\Delta\left(\frac{\omega}{\gamma}\right) = \left(\frac{\partial(\omega/\gamma)}{\partial H}\right) \Delta H + \left(\frac{\partial(\omega/\gamma)}{\partial \Theta}\right) \Delta \Theta, \quad (5)$$

where the first term characterizes in the field-swept FMR an effect of dragging magnetization M behind the applied field and the second term describes the fact that, in the field-swept experiment, magnetization undergoes an additional rotation $\Delta\Theta$ as the magnetic field is swept through resonance for a fixed Θ_H .²⁵

It can easily be shown that, for the thin films in the vicinity of a resonance,

$$\Delta\Theta \cong -\frac{\Delta H \sin(\Theta - \Theta_H)}{Q(\Theta_H)}. \quad (6)$$

On substituting Eq. (6) into Eq. (5), the transformation $\Delta H(\Theta_H) \rightarrow \Delta(\omega/\gamma)$ can be obtained in explicit form,

$$\Delta H(\Theta_H) = \frac{\Delta(\omega/\gamma)}{\left(\frac{\partial(\omega/\gamma)}{\partial H}\right) - \frac{\left(\frac{\partial(\omega/\gamma)}{\partial \Theta}\right) \sin(\Theta - \Theta_H)}{Q(\Theta_H)}}. \quad (7)$$

Hence, in accordance with Eq. (3), $\Delta H_{pp}^{\text{Gilb}}(\Theta_H)$ can be written in an expanded form of Suhl's formula,

$$\Delta H_{pp}^{\text{Gilb}}(\Theta_H) = \frac{\alpha}{\sqrt{3}} \frac{P(\Theta_H) + Q(\Theta_H)}{\left(\frac{\partial(\omega/\gamma)}{\partial H}\right) - \frac{\left(\frac{\partial(\omega/\gamma)}{\partial \Theta}\right) \sin(\Theta - \Theta_H)}{Q(\Theta_H)}}, \quad (8)$$

and, in accordance with Eqs. (1) and (4), the angular dependence $\Delta H_{pp}(\Theta_H)$ for a film with both intrinsic and extrinsic contributions is expressed as

$$\Delta H_{pp}(\Theta_H) = \frac{\left[\alpha + \frac{\Delta(\omega/\gamma)^{2\text{mag}}}{2(\omega/\gamma)}\right]}{\sqrt{3}} \frac{P(\Theta_H) + Q(\Theta_H)}{\left(\frac{\partial(\omega/\gamma)}{\partial H}\right) - \frac{\left(\frac{\partial(\omega/\gamma)}{\partial \Theta}\right) \sin(\Theta - \Theta_H)}{Q(\Theta_H)}}. \quad (9)$$

In order to extract the extrinsic contribution from the experimental dependence $\Delta H_{pp}^{\text{expt}}(\Theta_H)$, the inverse transformation can be performed:

$$\Delta(\omega/\gamma)^{2\text{mag}}(\Theta_H) = 2(\omega/\gamma) \frac{\sqrt{3}[\Delta H_{pp}^{\text{expt}}(\Theta_H) - \Delta H_{pp}^{\text{Gilb}}(\Theta_H)] \left[\frac{\partial(\omega/\gamma)}{\partial H} - \frac{\left(\frac{\partial(\omega/\gamma)}{\partial \Theta}\right) \sin(\Theta - \Theta_H)}{Q(\Theta_H)}\right]}{P(\Theta_H) + Q(\Theta_H)}, \quad (10)$$

where $\Delta H_{pp}^{\text{expt}}(\Theta_H)$ represents linear interpolation of the experimental data.²⁶ In accordance with Eq. (1), the fraction in Eq. (10) has the meaning of the dimensionless two-magnon damping constant with an angular dependence implicit in each term of the fraction.

III. EXAMPLES

The equality between the out-of-plane ΔH_{\perp} and in-plane ΔH_{\parallel} linewidths presents a clear evidence that the FMR linewidth is determined exclusively by the intrinsic contribution due to the Gilbert damping. However, it may happen that $\Delta H_{\perp} > \Delta H_{\parallel}$ or $\Delta H_{\perp} < \Delta H_{\parallel}$. In the former case, angular dependence $\Delta H(\Theta_H)$ can be complicated with a remarkably high ΔH_{\perp} .²¹⁻²⁴ Such a major deviation from the Gilbert phenomenological model is related to a specific granular microstructure characteristic of perpendicular media,^{22,23} polycrystalline ultrathin films with perpendicular surface anisotropy,^{21,24} or to polycrystalline multilayers with (possibly) discontinuous permalloy layers.^{7,8} The only exception to this rule is a copper-doped permalloy polycrystalline thin film with not specified microstructure.¹² The local resonance model with inhomogeneous broadening due to spatial variations in the perpendicular anisotropy²¹ or a combined model^{22,24} well account for angular dependence of the linewidth in the former case. The latter case (e.g., $\Delta H_{\perp} < \Delta H_{\parallel}$) is usually encountered in ultrathin films with a good structural order (e.g., epitaxial).^{10,15,16} In such a case, intrinsic (Gilbert) and extrinsic (two-magnon) contributions are usually more than sufficient to describe experimental data $\Delta H(\Theta_H)$.

Microscopic sources of the two-magnon scattering in ultrathin films have been described earlier and detailed information can be found in Refs. 3, 10, and 16. In this paper, we aim to show in a few examples a procedure of extracting the extrinsic contribution to the linewidth from

the experimental data using our approach and to compare its angular dependence with theoretical approaches within the framework of the two-magnon model without going into microscopic sources. Therefore, (i) we assume that ΔH_{\perp} is determined, but by the intrinsic Gilbert contribution; (ii) we evaluate $\Delta H_{pp}^{\text{extr}}(\Theta_H) = \Delta H_{pp}^{\text{expt}}(\Theta_H) - \Delta H_{pp}^{\text{Gilb}}(\Theta_H)$; (iii) we transform $\Delta H_{pp}^{\text{extr}}$ into $\Delta(\omega/\gamma)^{\text{extr}}$ vs Θ_H and $\Delta(\omega/\gamma)^{\text{extr}}$ vs Θ_H (or vs Θ); and (iv) we check if $\Delta(\omega/\gamma)^{\text{extr}}$ vs Θ_H (or vs Θ) is in agreement with the two-magnon model.

Figure 1(a) shows angular dependence of the FMR linewidth (open circles) of a sample 200 Pd/30 Fe/GaAs (001). The data are taken from Ref. 10. The numbers denote thickness in the units of atomic monolayers. The dotted line represents $\Delta H_{pp}^{\text{Gilb}}(\Theta_H)$ calculated from Eq. (8) with the following parameters: $f = 24$ GHz, $g = 2.02$, $4\pi M_{\text{eff}} = 20.6$ kG, $2K_1/M = 0.35$ kOe, and $\alpha = 0.0049$ that are nearly the same as in Ref. 10. The angular dependence of the extrinsic linewidth $\Delta H_{pp}^{\text{extr}}$ is shown by the dashed line. Using the inverse transformation [Eq. (10)], we can plot the frequency-swept linewidth $\Delta(\omega/\gamma)^{\text{Gilb}}$ and $\Delta(\omega/\gamma)^{\text{extr}}$ versus the field angle Θ_H or the magnetization angle Θ as it is shown by open circles in Figs. 1(a) and 1(b), respectively. It is worth noticing that, in accordance with Fig. 1(a), $\Delta(\omega/\gamma)^{\text{Gilb}}(\Theta_H) = 76$ and 120 Oe and $\Delta(\omega/\gamma)^{\text{extr}}(\Theta_H) = 0$ and 243 Oe, for $\Theta_H = 0^\circ$ and 90° , respectively, since they represent FWHM values. Comparison of $\Delta(\omega/\gamma)^{\text{Gilb}}$ and $\Delta(\omega/\gamma)^{\text{extr}}$ at $\Theta_H = 90^\circ$ clearly demonstrates the importance of the extrinsic contribution to the total linewidth.

While the angular dependence of $\Delta(\omega/\gamma)^{\text{Gilb}}$ is standard,⁶ the angular dependence of $\Delta(\omega/\gamma)^{\text{extr}}$ is worth commenting on. The plots of $\Delta(\omega/\gamma)^{\text{extr}}(\Theta_H)$ or $\Delta(\omega/\gamma)^{\text{extr}}(\Theta)$ [open circles in Figs. 1(b) and 1(c)] exhibit behavior predicted by the two-magnon model²⁰ with a characteristic decrease in the vicinity of $\Theta_H \lesssim 11^\circ$ and $\Theta \lesssim \pi/4$. Two-magnon scattering

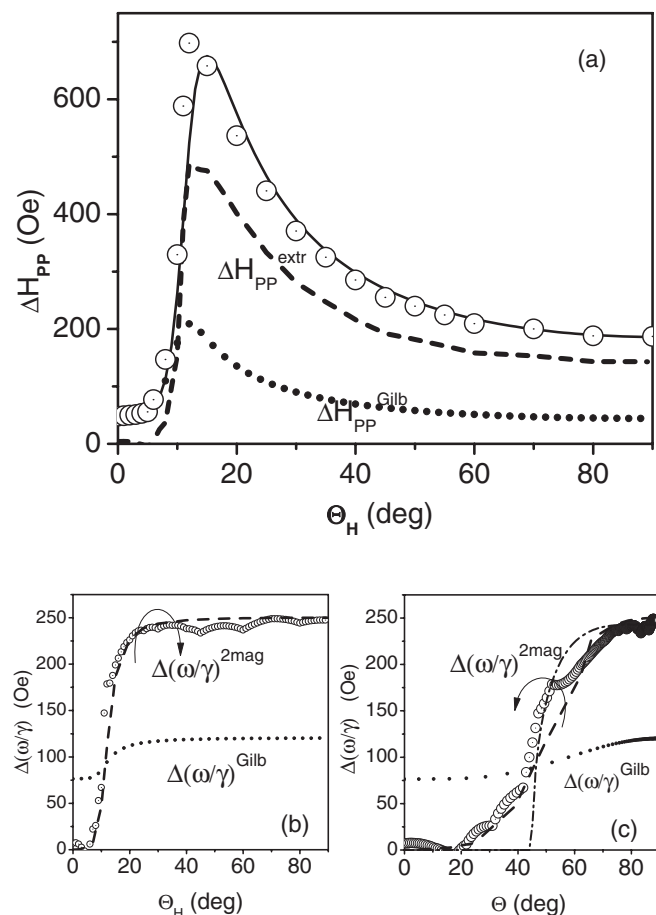


FIG. 1. (a) Measured (open circles) FMR linewidth ΔH_{pp} as a function of Θ_H for a sample 200Pd/30 Fe/GaAs (001). The data are taken from Ref. 10. Dotted line shows $\Delta H_{pp}^{Gilb}(\Theta_H)$ that was calculated on the basis of Eq. (8). Dashed line shows the linear interpolation of $\Delta H_{pp}^{extr}(\Theta_H) = \Delta H_{pp}^{exp}(\Theta_H) - \Delta H_{pp}^{Gilb}(\Theta_H)$. Solid line shows a fit to the experimental data with a sum of Gilbert and two-magnon contributions. (b) The frequency-swept (FWHM) linewidth as a function of Θ_H . Open circles and dots represent $\Delta(\omega/\gamma)^{extr}(\Theta_H)$ and $\Delta(\omega/\gamma)^{Gilb}(\Theta_H)$, respectively. Thick dashed line shows the results of numerical calculations. (c) The frequency-swept linewidth (open circles) as a function of magnetization angle Θ . Dash-dotted line shows the critical angle Ψ^{crit} as a function of Θ_H . Description of the other lines is the same as in (b).

theory describes the rate at which energy is transferred from the uniform precession to degenerate spin waves due to the presence of magnetic inhomogeneities and yields the two-magnon linewidth as a sum,

$$\Delta\omega^{2mag} = 2\pi |A_0|^2 \sum \delta(\omega_0 - \omega_{\mathbf{k}}), \quad (11)$$

where A_0 represents scattering amplitude and $\sum \delta(\omega_0 - \omega_{\mathbf{k}})$ is the density of degenerate spin waves with wave vector \mathbf{k} .²⁷ In ultrathin films, the two-magnon linewidth $\Delta(\omega/\gamma)^{2mag}$ as a function of Θ_H or Θ can be determined numerically from Eq. (11)^{20,23,24} or approximated analytically^{16,19,28} in a small

defect limit. In the last case, a simple expression has been proposed,¹⁹

$$\Delta(\omega/\gamma)^{2mag} \approx \frac{\langle \delta[\omega_{loc}(r)^2/\gamma^2] \rangle}{\delta(\omega_{ex}/\gamma)} \Psi^{crit}(\Theta_H), \quad (12)$$

where the leading term $\Psi^{crit}(\Theta_H) = \arcsin[(-P(\Theta_H)\cos 2\Theta / (P(\Theta_H) + 4\pi M)\sin^2\Theta)]^{1/2}$ (the expression is written in our coordinate system) is a critical angle—a stepwise function that switches off two-magnon scattering for $\Theta < \pi/4$. $\langle \delta\omega_{loc}(\mathbf{r})^2 \rangle$ is the square of local shift in resonance frequency due to inhomogeneity and $\delta\omega_{ex} = D\gamma(k)^2$ is the difference between the frequency of uniform precession and the frequency of a spin wave with the wave number k . D is the spin-wave stiffness constant. The fraction on the right side describes the fact that variations of the local inhomogeneous field due to defects $\delta(\omega_{loc}(\mathbf{r})/\gamma)$ are narrowed by exchange interactions represented by $\delta(\omega_{ex}/\gamma)$. If we take the spin-wave stiffness $D = 2.5 \times 10^{-9} \text{ G cm}^2$ for Fe and $k \approx 1/\xi$ with $\xi = 5 \text{ nm}$,¹⁰ the value of inhomogeneity field $\delta(\omega_{loc}/\gamma) \approx 1.6 \text{ kOe}$. This value seems to be reasonable for an inhomogeneous field created by misfit dislocations in an epitaxial Fe film of 30 ML.¹⁰

The dash-dotted line in Fig. 1(c) shows dependence (scaled) of Ψ^{crit} on Θ . It is seen that $\Delta(\omega/\gamma)^{extr}(\Theta)$ (open circles) is rather not well approximated by the analytical expression (12). Generally, the analytical expressions^{10,28,29} for $\Delta(\omega/\gamma)^{2mag}$ predict an abrupt disappearance of two-magnon scattering for $\Theta < \pi/4$. Numerical calculations¹⁹ explain such discrepancy as resulting from a finite Gilbert damping that leads to spin waves excited off resonance (see Fig. 5 in Ref. 19) and usually linewidth is finite at low Θ . We performed numerical calculations of the two-magnon contribution to the FMR linewidth as a sum over degenerate magnon states for various Θ_H in a similar way as described in Refs. 19 and 22. For this purpose, spin-wave manifold [see Eq. (11) in Ref. 19] for an Fe film with thickness $d = 30 \text{ ML}$ ($\sim 5 \text{ nm}$) and with exchange stiffness value $D = 2.5 \times 10^{-9} \text{ G cm}^2$ was determined versus wave number $0 < k < 3 \times 10^5 \text{ cm}^{-1}$ (i.e., $k^{\max}d < 0.2$) for field angle $0 < \Theta_H < 90$ and for microwave frequency $\omega/2\pi = 24 \text{ GHz}$ at $k = 0$. For each Θ_H , the density of degenerate states $\int_0^{k^{\max}} \delta(\omega_0 - \omega_{\mathbf{k}}) d\mathbf{k}$ was calculated assuming a finite intrinsic linewidth $2\alpha(\omega/\gamma)$ with $\alpha = 0.005$ and k -independent Gilbert damping. The results of numerical calculations are shown in Figs. 1(b) and 1(c) by the dashed lines. It is clearly seen that numerical calculation yields a finite two-magnon linewidth for small Θ_H in good agreement with the experimental data.³⁰

Two other examples concern $L2_1$ ordered Ni_2MnSn epitaxial films deposited by magnetron sputtering on MgO (100) substrates. Details on preparation, structural ordering, and magnetic properties can be found in Ref. 31. The most important feature of the Ni_2MnSn films in connection to FMR linewidth is that the spin-wave stiffness is of only $(8-9) \times 10^{-10} \text{ G cm}^2$, e.g., one of the lowest known for Heusler alloys.²⁶ As shown in Fig. 2(c), the low spin-wave stiffness of Ni_2MnSn results in a flattened spin-wave manifold in comparison to that of Fe, which have about three times higher spin-wave stiffness. This should result in a higher density of degenerate states than for Fe films. Since the

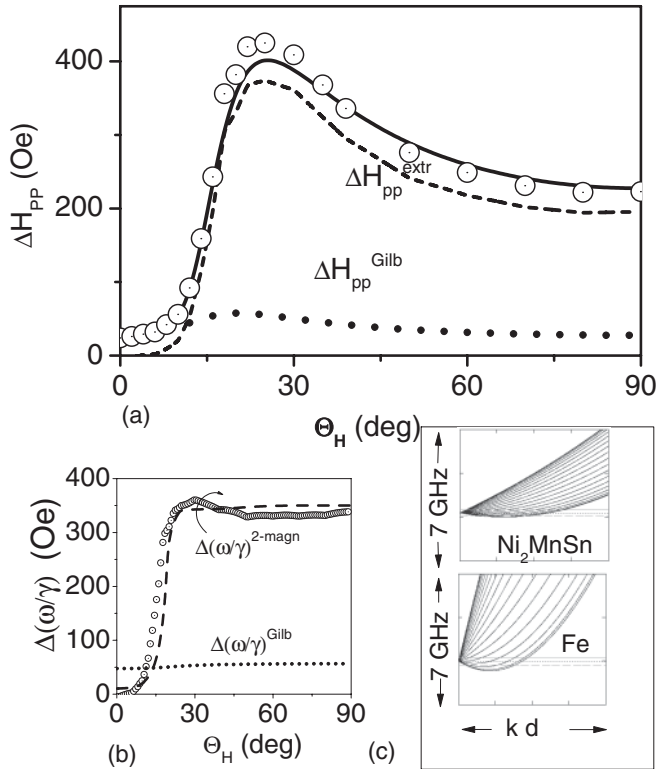


FIG. 2. (a) Measured (open circles) ferromagnetic resonance linewidth ΔH for a 30-nm $\text{Ni}_2\text{MnSn}/\text{MgO}$ (001) epitaxial film as a function of Θ_H . The dotted and dashed lines represent the intrinsic $\Delta H^{\text{Gilb}}(\Theta_H)$ and extrinsic $\Delta H^{\text{extr}}(\Theta_H)$ contribution, respectively. The solid line shows a fit to the experimental data with a sum of Gilbert and two-magnon contributions. (b) The frequency-swept linewidth $\Delta(\omega/\gamma)$ as a function of Θ_H . Open circles and dotted line in the inset represent the frequency-swept extrinsic and the Gilbert linewidth, respectively. The dashed line shows two-magnon contribution calculated numerically from spin-wave manifold. (c) Comparison of spin-wave manifold for ultrathin films of Ni_2MnSn and Fe of the same thickness of 6 nm. Magnetic field is applied in plane.

epitaxial films of Ni_2MnSn deposited at elevated temperature (in order to achieve good structural ordering) suffer from a relatively high roughness of 1–3 nm,³¹ two-magnon scattering is expected to be high in these films. Figure 2(a) shows angular dependence of the FMR linewidth (open circles) of a 30-nm-thick epitaxial film of Ni_2MnSn . Parameters used in our calculations are the following: $f = 9.38$ GHz, $g = 2.05$, $4\pi M_{\text{eff}} = 4.3$ kG, $2K_1/M = -0.05$ kOe, and $\alpha = 0.0075$. The most characteristic feature of the FMR linewidth is that the intrinsic Gilbert contribution (dotted line) is seven times smaller than the extrinsic contribution (dashed line) extracted according to our approach. Therefore, the angular dependencies $\Delta H(\Theta_H)$ and $(\Delta\omega/\gamma)(\Theta_H)$ (open circles) show that magnetization dynamics in Ni_2MnSn governed mostly by the extrinsic damping is probably due to the high surface roughness. Similar to the results shown in Fig. 1(b), Fig. 2(b) shows that the extrinsic damping is well described in terms of the two-magnon model. Numerical calculations of the two-magnon contribution based on spin-wave manifold of 30-nm-thick Ni_2MnSn film [Fig. 1(b), dashed line] trace quite well the extrinsic contribution.

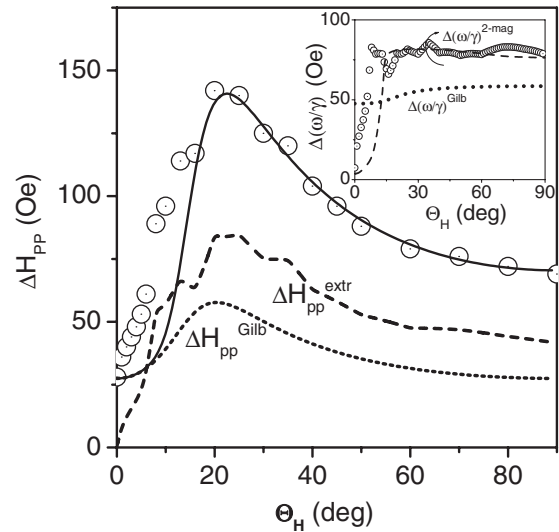


FIG. 3. Measured (open circles) ferromagnetic resonance linewidth ΔH for a 100-nm $\text{Ni}_2\text{MnSn}/\text{MgO}$ (001) epitaxial film as a function of Θ_H . The dotted and dashed lines represent the intrinsic $\Delta H^{\text{Gilb}}(\Theta_H)$ and extrinsic $\Delta H^{\text{extr}}(\Theta_H)$ contribution, respectively. The solid line shows a fit to the experimental data with a sum of Gilbert and two-magnon contributions. The inset shows the frequency-swept linewidth $\Delta(\omega/\gamma)$ as a function of Θ_H . Open circles and dotted line in the inset represent the frequency-swept extrinsic and intrinsic linewidth, respectively. The dashed line in the inset shows the two-magnon linewidth vs Θ_H calculated numerically (see text).

The described procedure for separating the extrinsic contribution from the experimental data not always leads to reasonable results that can be described exclusively by the two-magnon model for ultrathin films. Such a behavior is observed in some thicker Ni_2MnSn epitaxial films prepared by ultrahigh vacuum sputtering on MgO (100) substrates. The experimental data of FMR linewidth of a 100-nm-thick Ni_2MnSn is shown in Fig. 3 by open circles. The dotted curve shows angular dependence of the intrinsic contribution with $\Delta H^{\text{Gilb}}(90^\circ) = 26$ Oe that is comparable to the extrinsic one [$\Delta H^{\text{extr}}(90^\circ) = 50$ Oe] evaluated using our approach. The value of $\Delta H^{\text{Gilb}}(90^\circ) = 26$ Oe is rather small in accordance with that observed in other Heusler alloy films.^{18,32,33} Opposite to the results shown in Fig. 2, the extrinsic linewidth (inset in Fig. 3, open circles), which is comparable to the intrinsic contribution, shows no characteristic cutoff feature at $\Theta_H = 18^\circ$ ($\Theta = \pi/4$) predicted by the two-magnon model for ultrathin films. Using all needed parameters characterizing Ni_2MnSn film ($f = 9.08$ GHz, $g = 2.05$, $4\pi M_{\text{eff}} = 4.65$ kG, $2K_1/M = -0.08$ kOe, and $\alpha = 0.0075$), we calculated numerically the two-magnon contribution as a function of Θ_H performing integration over wave number range $0 < k < 3 \times 10^5 \text{ cm}^{-1}$. The dashed curve in the inset of Fig. 3 shows the results of calculations and it is clear that, at low angles Θ_H , the departure between experimental data and numerical calculations is substantial. In other words, in this case, the ultrathin film approach for two-magnon scattering cannot account for the observed angle dependence. Even though the microstructure of the 100-nm-thick Ni_2MnSn film is not known, the observed dependence of the FMR linewidth as a function of field angle may have as well a relationship with two-magnon scattering.

Qualitatively, following Hurben and Patton (see Fig. 15 in Ref. 3), such a course of the frequency-swept linewidth may arise from a mixed two-magnon scattering on isotropic (surface) defects and on spherical voids, which bring about a peak in ΔH^{extr} for low Θ_H .

IV. CONCLUSIONS

The out-of-plane angular dependence of FMR linewidth in thin films experiences a strong broadening if the magnetization is tilted from the normal to the film plane. We show that our expression for the field-swept linewidth, that may be regarded as the expanded Suhl's formula, explains this additional broadening without assuming distributions of local internal fields

and mosaicity in ultrathin magnetic films. A straightforward procedure of extraction of both the intrinsic and extrinsic contributions from the experimental data is presented with the extrinsic contribution well described in terms of the two-magnon scattering relaxation for ultrathin films. Angular dependence of the extrinsic contribution for the thicker film reveals departure from such a behavior. It can be qualitatively explained as resulting from two-magnon scattering on voids or other defects inside bulk of the thicker films.

ACKNOWLEDGMENT

This work was supported by the Polish Ministry of Science and Higher Education Grant No. 733/N-DAAD/2010/0.

*dubowik@ifmpan.poznan.pl

¹B. Heinrich, in *Ultrathin Magnetic Structures III, Fundamentals of Nanomagnetism*, edited by J. A. C. Bland and B. Heinrich (Springer-Verlag, Berlin, Heidelberg, 2005).

²A. G. Gurevich and G. A. Melkov, *Magnetization Oscillations and Waves* (CRC Press, Boca Raton, FL, 1996).

³M. J. Hurben and C. E. Patton, *J. Appl. Phys.* **83**, 4344 (1998).

⁴H. Suhl, *Phys. Rev.* **97**, 555 (1955).

⁵J. Smit and H. G. Beljers, Philips Res. Rep. **10**, 113 (1955).

⁶A. Z. Maksymowicz and K. D. Leaver, *J. Phys. F* **3**, 1031 (1973).

⁷S. Mizukami, Y. Ando, and T. Miyazaki, *Jpn. J. Appl. Phys.* **40**, 580 (2001).

⁸S. Mizukami, Y. Ando, and T. Miyazaki, *Phys. Rev. B* **66**, 104413 (2002).

⁹M. Jirsa, *Phys. Status Solidi B* **125**, 187 (1984).

¹⁰G. Woltersdorf and B. Heinrich, *Phys. Rev. B* **69**, 184417 (2004).

¹¹D. J. Twisselmann and R. D. McMichael, *J. Appl. Phys.* **93**, 6903 (2003).

¹²J. O. Rantschler, R. D. McMichael, A. Castillo, W. F. Egelhoff Jr., B. B. Maranville, D. Pulughurtha, A. P. Chen, and L. M. Connors, *J. Appl. Phys.* **101**, 033911 (2007).

¹³M. Farle, *Rep. Prog. Phys.* **61**, 755 (1998).

¹⁴W. Platow, A. N. Anisimov, G. L. Dunifer, M. Farle, and K. Baberschke, *Phys. Rev. B* **58**, 5611 (1998).

¹⁵Kh. Zakeri, J. Lindner, I. Barsukov, R. Meckenstock, M. Farle, U. von Hörsten, H. Wende, W. Keune, J. Rucker, S. S. Kalarickal, K. Lenz, W. Kuch, K. Baberschke, and Z. Frait, *Phys. Rev. B* **76**, 104416 (2007).

¹⁶J. Lindner, K. Lenz, E. Kosubek, K. Baberschke, D. Spoddig, R. Meckenstock, J. Pelzl, Z. Frait, and D. L. Mills, *Phys. Rev. B* **68**, 060102 (2003).

¹⁷M. Oogane, T. Wakitani, S. Yakata, R. Yilgin, Y. Ando, A. Sakuma, and T. Miyazaki, *Jpn. J. Appl. Phys.* **45**, 3889 (2006).

¹⁸M. Oogane, R. Yilgin, M. Shinano, S. Yakata, Y. Sakubara, Y. Ando, and T. Miyazaki, *J. Appl. Phys.* **101**, 09J501 (2007).

¹⁹R. D. McMichael and P. Krivosik, *IEEE Trans. Magn.* **40**, 2 (2004).

²⁰R. D. McMichael, D. J. Twisselmann, and A. Kunz, *Phys. Rev. Lett.* **90**, 227601 (2003).

²¹C. Chappert, K. L. Dang, P. Beauvillain, H. Hurdequint, and D. Renard, *Phys. Rev. B* **34**, 3192 (1986).

²²P. Krivosik, S. S. Kalarickal, Nan Mo, S. Wu, and C. E. Patton, *Appl. Phys. Lett.* **95**, 052509 (2009).

²³N. Mo, J. Hohlfeld, M. ul Islam, C. S. Brown, E. Girt, P. Krivosik, W. Tong, and C. E. Patton, *Appl. Phys. Lett.* **92**, 022506 (2008).

²⁴J.-M. Beaujour, D. Ravelosona, I. Tudosa, E. E. Fullerton, and A. D. Kent, *Phys. Rev. B* **80**, 180415 (2009).

²⁵C. Vittoria, R. C. Barker, and A. Yelon, *Phys. Rev. Lett.* **19**, 792 (1967).

²⁶The numerical code for exemplary calculations in MATHCAD is available upon request.

²⁷M. Sparks, R. Loudon, and C. Kittel, *Phys. Rev.* **122**, 791 (1999).

²⁸R. Arias and D. L. Mills, *Phys. Rev. B* **60**, 7395 (1999).

²⁹P. Landeros, R. E. Arias, and D. L. Mills, *Phys. Rev. B* **77**, 214405 (2008).

³⁰It is worth remarking that the results of numerical calculations may be quite well approximated by a normalized adjusted function $\Delta(\omega/\gamma)(\Theta_H) = \Delta(\omega/\gamma)(\pi/2) \{1 - 1/[1 - (\Theta_H/B)^n]\}$, where B is an angle Θ_H corresponding to a cutoff magnetization angle $\Theta = \pi/4$ and n is a number in a range of 6–10 that determines the slope at the cutoff angle B . For the data presented in Fig. 1, $B = 0.19$ rad and $n = 6$.

³¹J. Dubowik, I. Gościńska, K. Załęski, and H. Głowiński (accepted to Acta Phys. Pol. A).

³²B. Heinrich, G. Woltersdorf, R. Urban, O. Mosendz, G. Schmidt, P. Bach, L. Molenkamp, and E. Rozenberg, *J. Appl. Phys.* **95**, 7462 (2004).

³³S. Mizukami, D. Watanabe, M. Oogane, Y. Ando, Y. Miura, M. Shirai, and T. Miyazaki, *J. Appl. Phys.* **105**, 07D306 (2009).